Molecular Microbiology (2006) doi:10.1111/j.1365-2958.2006.05184.x

A new FtsZ-interacting protein, YlmF, complements the activity of FtsA during progression of cell division in *Bacillus subtilis*

Shu Ishikawa,† Yoshikazu Kawai,† Konosuke Hiramatsu, Masayoshi Kuwano and Naotake Ogasawara*

Graduate School of Information Science, Nara Institute of Science and Technology, 8916-5 Takayama, Ikoma, Nara 630-0101, Japan.

Summary

The assembly of ring-like structures, composed of FtsZ proteins (i.e. the Z ring), is the earliest and most essential process in bacterial cytokinesis. It has been shown that this process is directly regulated by the FtsZ-binding proteins, FtsA, ZapA, and EzrA, in *Bacillus subtilis*. In this study, protein complexes that are involved in Z-ring formation were chemically cross-linked *in vivo*, purified by affinity chromatography, and analysed by mass spectrometry. Analysis of the results identified YlmF as a new component of the FtsZ complex. Yeast two-hybrid analysis and fluorescence microscopy of YFP–YlmF in *B. subtilis* cells indicated YlmF localizes to the division site in an FtsZ-dependent manner. A single disruption of YlmF resulted in a slight elongation of cells; however, simultaneous inactivation of both YlmF and FtsA showed synthetic lethality caused by complete blockage of cell division due to the defect in Z-ring formation. In contrast, the *ftsA*-null mutant phenotype, caused by inefficient Z-ring formation, could be complemented by overexpression of YlmF. These results suggest that YlmF has an overlapping function with FtsA in stimulating the formation of Z rings in *B. subtilis*.

Introduction

Cell division is a tightly regulated process that ensures accurate and efficient segregation of chromosomal material and maintains both cell size and shape. The FtsZ protein is a bacterial tubulin homologue that has the ability to polymerize and form a ring-like structure (the Z ring) at sites of cell division (Errington *et al*., 2003). Z-ring formation is the earliest event identified in the progression of bacterial cell division. The Z ring is required for the recruitment of other cell division proteins and serves as a framework for assembly of the cell division machinery (Errington *et al*., 2003; Romberg and Levin, 2003). In *Escherichia coli* and *Bacillus subtilis*, the Z ring has been shown to recruit 13 and 10 cell division proteins, respectively, to the sites of cell division directly or indirectly (Gueiros-Filho and Losick, 2002; Errington *et al*., 2003; Haeusser *et al*., 2004; Aarsman *et al*., 2005).

In *E. coli*, both FtsA and ZipA have been shown to interact directly with FtsZ and to be the first proteins recruited to the Z ring (Errington *et al*., 2003; Romberg and Levin, 2003). They are essential for cellular growth and recruitment of cell division proteins to cell division sites at later stages of cell division (Lutkenhaus and Donachie, 1979; Hale and de Boer, 1997; Wang *et al*., 1997; Pichoff and Lutkenhaus, 2002). Both proteins localize to the Z ring independently in an FtsZ-dependent manner; Z-ring formation also occurs in cells in which either protein is lacking but results in an inactive structure. However, in the absence of both proteins, FtsZ fails to form the Z ring and instead appears as spots on fluorescence microscopy at expected sites of cell division (Pichoff and Lutkenhaus, 2002). These observations suggest that FtsA and ZipA have overlapping roles in the maintenance of Z-ring integrity (Pichoff and Lutkenhaus, 2002). Moreover, a single residue change in the FtsA protein bypasses the requirement for ZipA without changing the cellular growth rate, supporting the premise that these proteins have overlapping roles (Geissler *et al*., 2003).

On the other hand, *B. subtilis* has no ZipA homologue but possesses three FtsZ-interacting proteins, FtsA, ZapA and EzrA (Errington *et al*., 2003). The *B. subtilis* FtsA protein has been shown to interact directly with FtsZ (Wang *et al*., 1997; Jensen *et al*., 2005) and to localize to sites of cell division (Feucht et al., 2001). However, in contrast to *E. coli*, *ftsA* can be disrupted in *B. subtilis*, even though *ftsA*-null mutants showed a severe deficiency in cell division (Beall and Lutkenhaus, 1992; Jensen *et al*., 2005). In the absence of FtsA, FtsZ appears primarily as

Accepted 30 March, 2006. *For correspondence. E-mail nogasawa@bs.naist.jp; Tel. (+81) 743 72 5430; Fax (+81) 743 72 5439. †S.I. and Y.K. contributed equally to this work.

diffuse bands at regular intervals and the proportion of normal Z-ring formation is reduced to about 10% of wild-type cells, suggesting a critical role for FtsA in Z-ring formation in *B. subtilis* (Jensen *et al*., 2005). ZapA was identified as a factor that suppressed the lethality of the overexpression of the cell division inhibitor, MinD (Gueiros-Filho and Losick, 2002). ZapA protein binds directly to FtsZ and promotes bundling of either the FtsZ monomer or FtsZ protofilaments *in vitro* (Gueiros-Filho and Losick, 2002). EzrA has been proposed to be as a negative regulator of Z-ring formation. Cells lacking EzrA formed Z rings at the cell poles as well as medial sites, and lowered the critical concentration of FtsZ required for ring formation (Levin *et al*., 1999). EzrA protein directly interacts with FtsZ to prevent its assembly *in vitro*, possibly by blocking subunit addition or inhibiting lateral interactions of FtsZ filaments (Haeusser *et al*., 2004). In addition, we have reported recently that EzrA and FtsL, an essential late-stage cell division protein, promote Z-ring dissociation and constriction at medial division sites with a partly complementary function (Kawai and Ogasawara, 2006). Although ZapA and EzrA are both dispensable for cell growth and cell division in *B. subtilis*, the simultaneous depletion of both proteins results in a severe block of cell division, indicative of their participation in the *B. subtilis* cell division process (Gueiros-Filho and Losick, 2002).

The assembly of cell division proteins at sites of cell division has been studied primarily by examining the dependence of protein localization on other cell division proteins as well as by two-hybrid analysis. In order to examine the interactions between cell division proteins directly in living cells, in the present study we developed a method to isolate protein complexes *in vivo* using histidine tags fused to the gene of interest and to identify the proteins in these isolated complexes by mass spectrometry. By adopting this method, we demonstrated the association of FtsZ, FtsA, ZapA and EzrA *in vivo*. Furthermore, we identified the YlmF protein as a new component of this complex. It was suggested that YlmF is involved in cell division because a YlmF mutant resulted in the abnormal morphology of *Streptococcus pneumoniae* cells (Fadda *et al*., 2003). Interestingly, YlmF is conserved in bacteria that have no FtsA homologue and has been demonstrated to be essential for cellular growth in *Synechococcus elongatus* PCC 7942 (Miyagishima *et al*., 2005) without FtsA homologue, suggesting a functional relationship between FtsA and YlmF. Indeed, we found that deletion of YlmF in FtsA-depleted *B. subtilis* cells resulted in a complete inhibition of Z-ring formation and cell division. Additionally, overexpression of YlmF in FtsA-deleted cells suppressed the division defect associated with deletion of FtsA. Thus, we demonstrated that YlmF has an overlapping role with FtsA in the formation of Z rings in *B. subtilis*. Based on these new findings, the mechanism of early-stage cell division will be discussed.

During preparing this manuscript, it has been suggested that YlmF (renamed SepF) is required for proper execution of septum synthesis in *B. subtilis* (Hamoen *et al*., 2005). We also discussed relevance of our findings to their results.

Results

Identification of YlmF as a component of the FtsZ complex

To detect protein–protein interactions in which FtsZ and the FtsZ-associated proteins, FtsA, ZapA and EzrA, are involved *in vivo*, we constructed *B. subtilis* strains that had histidine tags fused to the 3′ end of each gene on the chromosome. Construction was performed by integrating the pMUTinHis derivatives as shown in Fig. 1A. The resultant strains, 168ezrAHis, 168ftsZHis, 168ftsAHis and 168zapAHis, grew at the similar rate with that of parental wild-type strain, although partial impairment of the function was observed for FtsA-His as described in *Experimental procedures*. To examine the expression of histidine-tagged proteins in the mutant strains, Western blotting analysis was performed using anti-His-tag antibody, and the amount of FtsZ-, FtsA- and EzrA-His molecules per cell were estimated to be 4400, 970 and 6100 respectively (Fig. S1). Cellular amount of FtsZ and FtsA has been reported to be 5000 and 1000 molecules respectively (Feucht *et al*., 2001), indicating that His-tag fusion did not affect the expression level significantly for FtsZ and FtsA.

To avoid dissociation of interactions during the purification process, protein complexes were cross-linked using a membrane-permeable cross-linker, formaldehyde, as described previously, with modifications (Layh-Schmitt *et al*., 2000; Vasilescu *et al*., 2004). Protein complexes were then purified using Ni resin, followed by the passage through a Microcon-100 column to remove proteins with molecular masses lower than 100 kDa, and the high molecular complexes were separated using SDS-PAGE after heating to disrupt cross-linked proteins. Although both purity and quantity of the isolated complexes were dependent on the bait proteins, the protein complex purified using FtsA as bait showed, in addition to background bands, clear specific bands by SDS-PAGE (Fig. 1B). Thus, we used the complex for mass spectrometric analysis to identify proteins specifically involved in the complex of FtsZ and the FtsZ-associated proteins. In order to distinguish the specific protein from non-specific backgrounds, we analysed in parallel the complex isolated by using DnaC [a component of replisome, interacting with DnaI (Imai *et al*., 2000; Bruand *et al*., 2001)] as bait (Fig. 1B). All visible bands from the two complexes were subjected

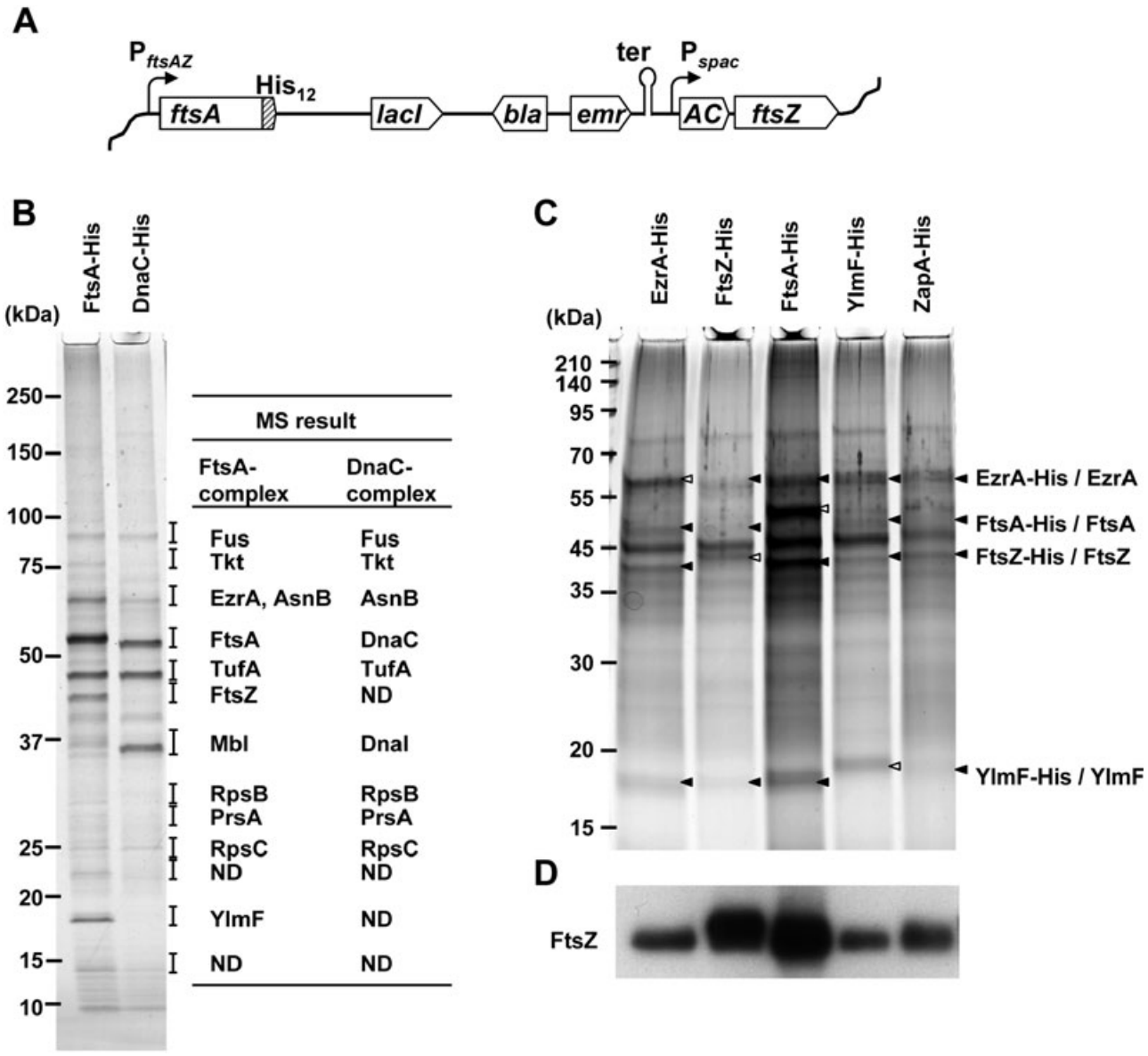

Fig. 1. Isolation and analysis of the protein complexes involved in Z-ring formation.

A. Schematic representation of the *ftsAZ* region of the FtsA-His expression strain (168ftsAHis) used for purification of the FtsA complex. Note that this strain was cultured in the presence of 1 mM IPTG to induce *ftsZ* expression from the *spac* promoter (P_{spac}). His12: coding sequence of 12 histidines. *lacI*: repressor gene for P_{spac}. *bla*: ampicillin-resistance gene (beta-lactamase). *emr*: erythromycin-resistance gene. ter: *E. coli* terminator *rrnB*. *AC*: C-terminal region of *ftsA*.

B. SDS-PAGE of FtsA and DanC complexes. The FtsA and DnaC complexes, purified from 30 OD_{600} units of 168ftsAHis and 168dnaCHis cells, respectively, were separated by 4–20% gradient SDS-PAGE and visualized by silver staining. All distinguishable bands were analysed by mass spectrometry as described in *Experimental procedures*. The width of gel slices used for the analysis is indicated by bars at the right of gel image, and the proteins from which more than two peptides were detected by mass spectrometry are indicated. M, protein standards; ND, no protein was detected.

C. The EzrA, FtsZ, FtsA, YlmF and ZapA complexes, purified from 4, 4, 36, 56 and 54 OD_{600} units of 168ezrAHis, 168ftsZHis, 168ftsAHis, 168ylmFHis and 168zapAHis cells, respectively, were separated by 4–20% gradient SDS-PAGE after heating and visualized by silver staining. Positions, corresponding to native and histidine-tagged proteins, are indicated by filled and open arrowheads on the gel respectively. M, protein standards.

D. FtsZ in the EzrA, FtsZ, FtsA, YlmF and ZapA complexes were detected by Western blotting using anti-FtsZ serum. The same amount of proteins as in panel C was analysed.

to in gel trypsin digestion, followed by liquid chromatography-tandem mass spectrometry (LC-MS/MS) analysis, and we could assign specific proteins in most of them. Several proteins abundant in cells were simultaneously identified in both samples, and they were also copurified in other protein complexes [e.g. RpoC (beta subunit of RNA polymerase), SigA (housekeeping sigma factor) and OdhB (small subunit of 2-oxoglutarate dehydrogenase (S. Ishikawa and N. Ogasawara, unpubl. data)], indicating that they were non-specific backgrounds. Thus, we concluded that FtsA, FtsZ, EzrA, YlmF and Mbl would form a complex *in vivo*. YlmF is a 17 kDa protein with unknown function in *B. subtilis*, and Mbl is a cell shape determining protein (Jones *et al*., 2001; Daniel and Errington, 2003). Their interaction with cell division proteins has not been reported yet.

Furthermore, specific bands corresponding to FtsA, FtsZ, EzrA and YlmF, but not to Mbl, were observed in protein complexes that were isolated using FtsZ, ZapA and EzrA as baits, although some of the bands were not clear and the confirmation by mass spectrometry has not been performed yet (Fig. 1C). Detection of possible EzrA, FtsA, FtsZ and YlmF bands in the ZapA complex, strongly suggested the existence of ZapA in the *in vivo* complex of early cell division proteins, although ZapA could not be detected by mass spectrometry. Additionally, we constructed the strain expressing YlmF-His (168ylmFHis) and detected the bands corresponding to EzrA, FtsA and FtsZ in the YlmF complex (Fig. 1C). Finally, Western blotting analysis using anti-FtsZ antibody showed that all complexes contained FtsZ (Fig. 1D).

In sum, our complex analysis demonstrated that FtsZ, FtsA, EzrA and ZapA could be isolated as a complex *in vivo*. In addition, we also identified YlmF as a new component of the complex. Identification of Mbl in the complex using FtsA as bait is intriguing, but we did not further validate the result in this study.

Direct interactions among FtsA, EzrA and ZapA have not been demonstrated. Thus, in the complex we isolated, they will bind to FtsZ filaments without contact between them. To determine the protein YlmF directly interacts within the FtsZ complex, we performed yeast two-hybrid analyses. For this purpose, we fused each protein-encoding gene to the DNA-binding and activator domains of the GAL4 gene in pGBT9 and pAD424 respectively. Interactions were assessed by expression of the *HIS3* reporter gene as described in *Experimental procedures* (Fig. 2). In our assay, the interaction between FtsZ and EzrA, which has been demonstrated by *in vitro* cross-linking experiments (Haeusser *et al*., 2004), and the dimmer formation of FtsA, which has been shown *in vitro* and *in vivo* (Feucht *et al*., 2001), could not be detected. We, however, demonstrated the following known interactions: FtsZ–FtsZ, FtsZ–FtsA and FtsZ–ZapA (Wang *et al*., 1997; Gueiros-Filho and Losick, 2002), although the self interaction of FtsZ seemed to be quite week in our assay comparing with a previous yeast two-hybrid analysis (Wang *et al*., 1997). Furthermore, we found that YlmF has the ability to interact with FtsZ and to form a YlmF–YlmF dimer.

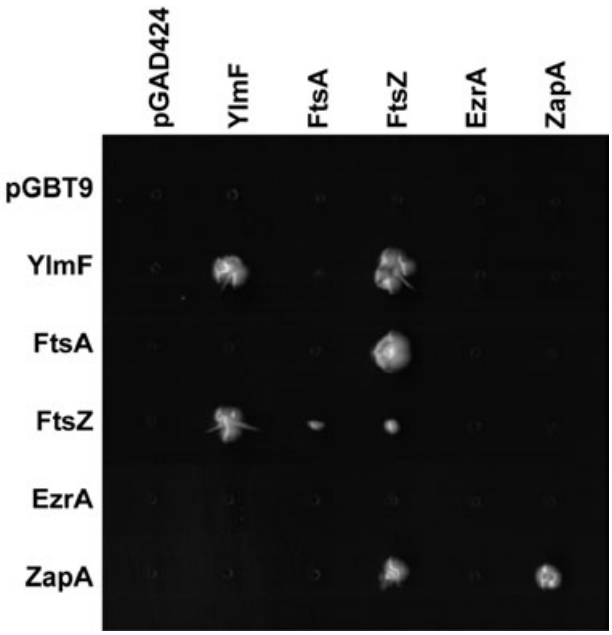

Fig. 2. Yeast two-hybrid analysis of interactions between FtsZ and FtsZ-associated proteins. Diploid strains were obtained by mating PJ69-4A-containing pGBT9 derivatives with PJ69-4a-containing pGAD424 derivatives. Interactions between proteins were detected on selection medium (SC-LWH) supplemented with 5 mM 3-AT after 5 day incubation.

FtsZ-dependent localization of YlmF at sites of cell division

To determine the localization of YlmF to sites of cell division, we fused the *yfp* gene, under the control of the IPTG-inducible *spac* promoter (P_{spac}), to the 5′-terminus of the *ylmF* gene and integrated this construct into the *aprE* locus of *B. subtilis* CRK6000. Fluorescence microscopy of YFP–YlmF-expressing cells, YK203 (*aprE*::P_{spac}-*yfp-ylmF*), revealed transverse bands in the middle of the cells (Fig. 3A), indicating that YlmF indeed localizes to sites of cell division. To examine the dependence of YlmF localization on FtsZ, we introduced *yfp-ylmF* into a temperature-sensitive mutant of *ftsZ*, *ts1*(*ftsZ1*) (Callister *et al*., 1983), in which FtsZ localization became diffused between nucleoids at the non-permissive temperature (Michie *et al*., 2006), and the resultant strain [YK199; *ts1*(*ftsZ1*) *aprE*::P_{spac}-*yfp-ylmF*] was examined at both the permissive (30°C) and non-permissive (48°C) temperatures. The results revealed that localization of YFP–YlmF, observed at sites of cell division at the permissive

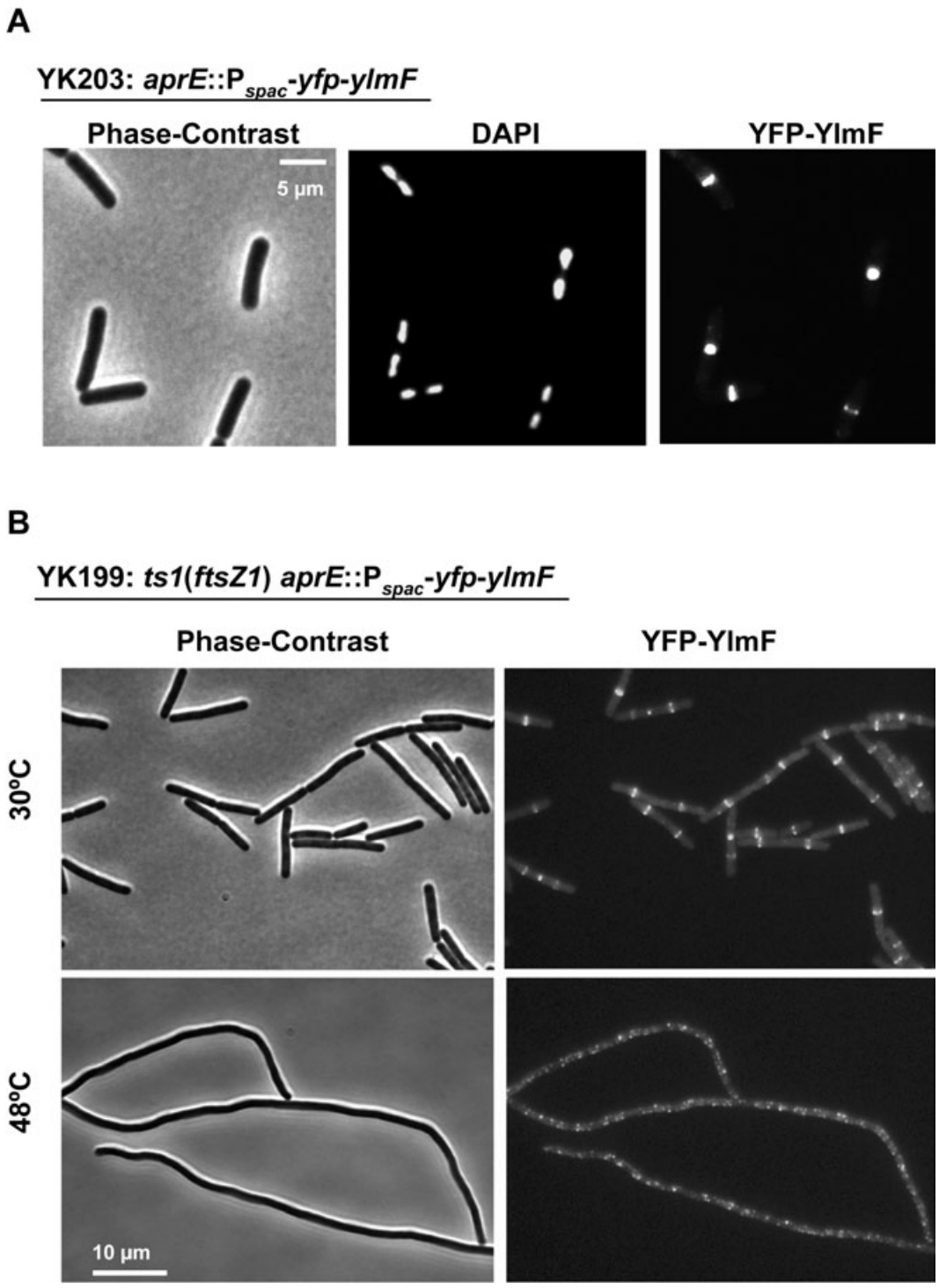

Fig. 3. FtsZ-dependent localization of YFP–YlmF fusion proteins.
A. Phase-contrast, DAPI-stained nucleoids and YFP fluorescence images of YK203 cells (*aprE*::P_{spac}-*yfp-ylmF*) from exponentially growing cultures in PAB medium with 1 mM IPTG at 37°C.
B. YK199 cells [*ts1*(*ftsZ1*) *aprE*::P_{spac}-*yfp-ylmF*] were grown to exponential phase (OD_{600} = 0.1) in LB medium supplemented with 1 mM IPTG at 30°C. Phase-contrast and YFP fluorescence images were captured at 0 and 90 min after temperature shift up from 30°C to 48°C.

temperature, was dispersed in filamentous cells during the 90 min period after a shift to the non-permissive temperature (Fig. 3B). Thus, we concluded that YlmF localizes to sites of cell division in an FtsZ-dependent manner.

Partial impairment of cell division in the ylmF*-null mutant*

To investigate the role of YlmF in cell division, we constructed a deletion mutant of *ylmF* by replacing *ylmF* with the spectinomycin-resistance gene to create strain YK204 (*ylmF*::*spec*). The growth rate of YK204 cells appeared normal under the growth conditions examined [minimal or PAB medium at 25, 30, 37 and 45°C (data not shown)], although the cells were slightly elongated compared with parental cells (CRK6000). The average cell length of the YK204 and parental cells was 5.4 ± 1.3 μm (average of 504 cells) and 4.1 ± 1.0 μm (average of 503 cells) respectively.

The sequence of the *B. subtilis* genome suggested that *ylmF* is the third gene in an operon whose order is *ylmD*, *ylmE*, *ylmF*, *ylmG*, *ylmH* and *divIVA*. DivIVA is responsible for the localization of the MinCD complex to the poles of the cell, to inhibit Z-ring formation there (Marston *et al*., 1998); its absence impairs cell division (Cha and Stewart, 1997; Edwards and Errington, 1997). To eliminate the possibility that the slight cell elongation caused by the disruption of *ylmF* was due to an effect on downstream gene expression, we introduced a xylose-inducible copy of *ylmF*, P_{xyl}-*ylmF*, into the *amyE* locus of YK204. When the resulting YK205 cells (*ylmF*::*spec amyE*::P_{xyl}-*ylmF*) were cultured in the absence of xylose, the average cell length was 5.4 ± 1.2 μm (average of 503 cells). In contrast, in the presence of 1% xylose, the average cell length was reduced to 4.1 ± 0.8 μm (average of 503 cells), comparable to that of wild-type cells. In agreement with this observation, Affymetrix DNA-chip analysis revealed that the expression level of *ylmF* from the *xyl* promoter became comparable with that from the native *ylmF* promoter after 60 min incubation in the presence of 1% xylose (data not shown). These results suggest that inactivation of YlmF indeed results in a partial impairment of cell division.

Effect of the ylmF*-null mutation in cells with reduced concentrations of FtsA*

In *E. coli*, FtsA is essential for cell division (Lutkenhaus and Donachie, 1979). In contrast, *B. subtilis ftsA*-null strains were viable, although they grew slowly and became extremely filamentous during vegetative growth (Beall and Lutkenhaus, 1992; Jensen *et al*., 2005). It was reported that disruption of *ylmF* results in a partial cell division defect in affected strains of *S. pneumoniae* (Fadda *et al*., 2003), belonging to Firmicutes possessing both *ftsA* and *ylmF*. Recently, a YlmF homologue present in the Cyanobacterium, *S. elongatus* PCC 7942, was found to be essential for cell division and viability (Miyagishima *et al*., 2005). Interestingly, no *ftsA* homologue has been identified in any Cyanobacterial genome to date, although both *ylmF* and *ftsZ* have been found in all Cyanobacteria. These results prompted us to investigate the functional relationships between YlmF and FtsA in *B. subtilis*.

We therefore examined the effects of the absence of YlmF on cell division under conditions where the cellular FtsA were depleted. In addition, we examined the effects of the inactivation of either ZapA or EzrA under those same conditions. These experiments were accomplished by introducing disrupted *ylmF*, *zapA* or *ezrA* genes into strain MD133 (*ftsA*::*cat aprE*::P_{spac}-*ftsA*) in which *ftsA* at native position had been replaced with promoter- and terminator-less *cat* gene to ensure the FtsZ expression from the native promoter and the ectopic FtsA expression is dependent on the *spac* promoter (M. Yoshimura and N. Ogasawara, unpublished). In agreement with the viability of *ftsA*-deleted strains, MD133 cells were able to grow on Luria–Bertani (LB) plate in the absence of IPTG (i.e. in the absence of FtsA), although they formed long filaments (data not shown), as shown in Fig. 4A. In contrast, the *ylmF*-disrupted derivative (YK200; *ftsA*::*cat aprE*::P_{spac}-*ftsA ylmF*::*spec*) became unable to grow in the absence of IPTG. The inactivation of *zapA* and *ezrA* did not affect growth at the same condition respectively.

To examine cell division in the *ftsA ylmF* double mutant cells, YK200 cells were first cultured in LB liquid medium containing 1 mM IPTG, transferred into medium without IPTG, and changes in cell morphology after 90 min incubation in the absence of IPTG were examined. In the presence of IPTG, the cell length of control MD133 cells and YK200 cells was comparable (Fig. 4B). In contrast, after 90 min incubation in the absence of IPTG, the YK200 cells appeared as long filaments with lysed cells, even though FtsA was not completely depleted in this condition in MD133 cells, judging from their mild cell elongation compared with that of the *ftsA*-depleted cells (see Fig. 6).

Although we have not as yet determined the cellular amount of FtsA in these mutants because of unavailability of appropriate antibody, our results suggested that the absence of YlmF causes severe division defect and lethality in cells lacking or producing a limited amount of FtsA.

Z-ring formation in ftsA *and* ylmF *double mutant*

It has been suggested that FtsA is critical for the efficient formation of functional Z rings (Jensen *et al*., 2005). Our results suggest that YlmF also acts in Z-ring formation. To investigate this possibility, we carried out immunofluorescence microscopy with antibodies against FtsZ in the *ftsA ylmF* double mutant (YK200, *ftsA*::*cat aprE*::P_{spac}-*ftsA*

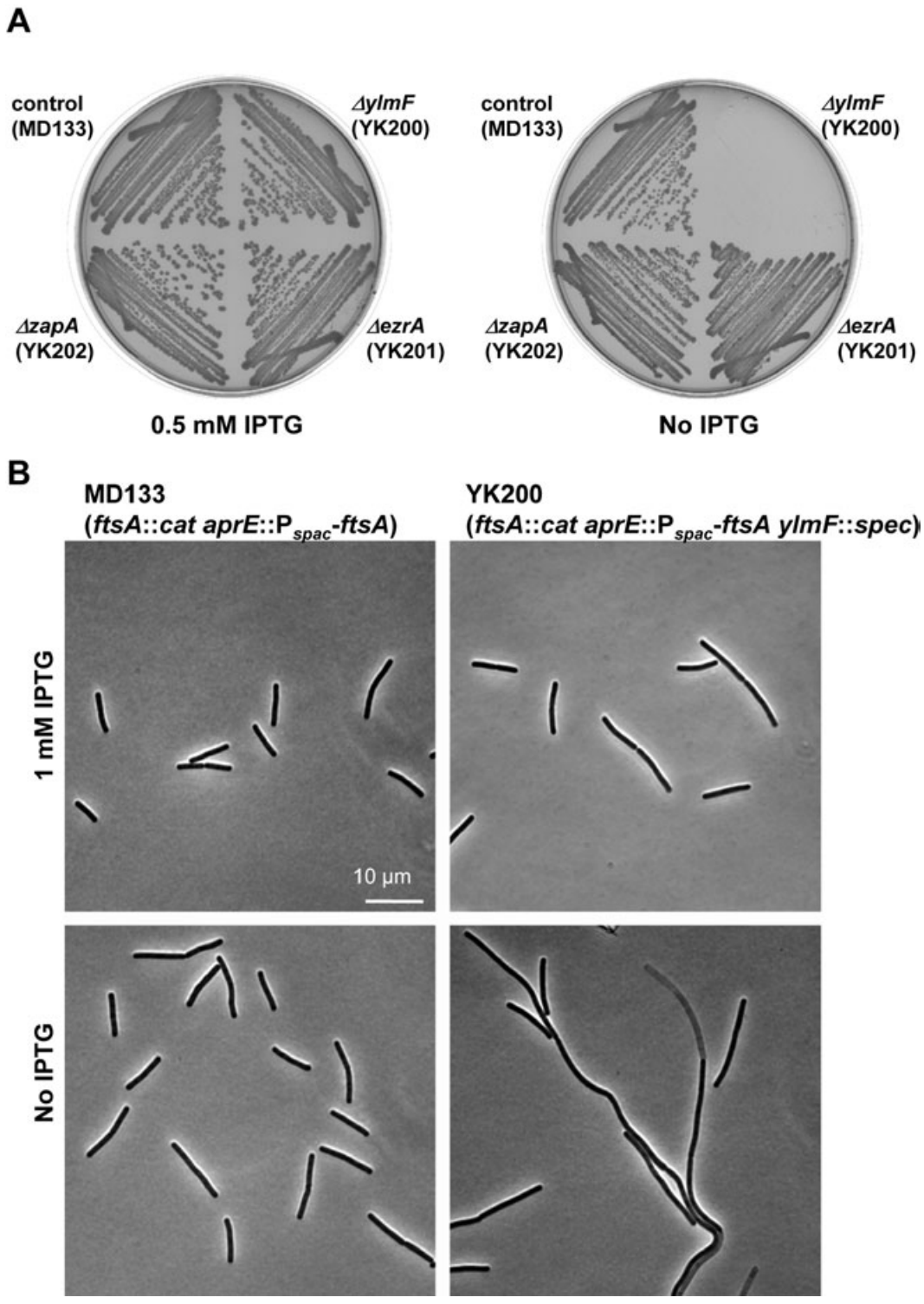

Fig. 4. Effects of reduced levels of FtsA on growth of *ylmF*-, *ezrA*- and *zapA*-inactivated cells.
A. Growth of *ylmF*, *ezrA* and *zapA* deletion mutants was assayed when expression of FtsA was reduced. Control, Δ*ylmF*, Δ*ezrA* and Δ*zapA* represent MD133 (*ftsA*::*cat aprE*::P_{spac}-*ftsA*), YK200 (*ftsA*::*cat aprE*::P_{spac}-*ftsA ylmF*::*spec*), YK201 (*ftsA*::*cat aprE*::P_{spac}-*ftsA ezrA*::*spec*), and YK202 (*ftsA*::*cat aprE*::P_{spac}-*ftsA zapA*::*spec*) cells respectively. The strains were grown on LB supplemented with 1 mM IPTG, inoculated onto LB plates with 0.5 mM or without IPTG, and subsequently incubated overnight at 30°C before photography.
B. MD133 (control) and YK200 (Δ*ylmF*) cells, grown to mid-exponential phase (OD_{600} = 0.3) in LB medium supplemented with 1 mM IPTG at 30°C, were inoculated into LB medium without IPTG to a get a final OD_{600} of 0.03 and were subsequently cultured at 30°C for 90 min. Phase-contrast images were captured at 0 and 90 min after the removal of IPTG.

ylmF::*spec*). In the control strain MD133 (*ftsA*::*cat aprE*::P_{spac}-*ftsA*), after 90 min incubation in the absence of IPTG, typical Z ring (sharp band) was still observed in the cells (Fig. 5A, d–f). In contrast, in YK200 cells cultivated at the same condition, FtsZ localization became dispersed in nucleoid free regions of filamentous cells and the remaining Z rings became abnormal spiral-like structure (Fig. 5A, j–l).

These results indicated that simultaneous absence of FtsA and YlmF indeed resulted in a severe inhibition of Z-ring formation. To further examine this possibility, we constructed a new double mutant, whose viability is maintained by inducible copy of YlmF. To this end, we constructed a new *ftsA*-null strain in which the entire *ftsA* sequence was substituted by *erm* (erythromycin-resistance gene) and the *spac* promoter ensuring expression of the downstream *ftsZ* gene (YK206, *ftsA*::*erm* P_{spac}-*ftsZ*). YK206 grew in the absence of IPTG because the *lacI* gene was not present in this strain, and thus, *ftsZ* is expressed constitutively. Then we introduced an inducible copy of *ylmF*, P_{xyl}-*ylmF*, into the *amyE* locus of YK206 and replaced the *ylmF* gene with a spectinomycin-resistance gene. The resulting strain YK210 (*ylmF*::*spec ftsA*::*erm* P_{spac}-*ftsZ amyE*::P_{xyl}-*ylmF*) grew in the presence of xylose (i.e. in the presence of YlmF). Furthermore, we found that the impairment of cell division due to the FtsA inactivation was partially corrected (Fig. 5B, a–c), as discussed in the next section. In contrast, when xylose was withdrawn (i.e. when YlmF was depleted), cell division was inhibited and long filaments developed. Furthermore, strong inhibition of Z-ring formation was observed in the long filaments of YK210 cells and no typical Z ring (sharp band) became detectable (Fig. 5B, d–j).

We examined FtsZ levels in MD133, YK200 and YK210 cells, and they were not affected by withdrawal of IPTG or xylose, although somewhat changed compared with parental wild-type cells (Fig. 5C). These observations strongly suggest that monomers or protofilaments are not organized into the functional Z-ring structure at division sites in the absence of both FtsA and YlmF in *B. subtilis* cells, resulting in complete inhibition of cell division. Similar FtsZ localization pattern has been observed in *E. coli* cells in the absence of both ZipA and FtsA, which have overlapping roles in the formation and stabilization of the Z ring (Pichoff and Lutkenhaus, 2002).

Complementation of the ftsA*-null phenotype by overexpression of YlmF*

Complete inhibition of Z-ring formation by simultaneous inactivation of FtsA and YlmF suggests their overlapping roles in the progression of cell division. Furthermore, the filamentous phenotype due to the *ftsA* inactivation was apparently suppressed by the overexpression of YlmF in YK210 cells (Fig. 5B). Therefore, we further examined the ability of YlmF to complement impairment of cell growth and division in the *ftsA*-null mutant. As observed in the *ftsA*-null mutants, YK206 cells (*ftsA*::*erm* P_{spac}-*ftsZ*), grew at half the parental rate (increase in OD_{600}, Fig. 6A), were approximately three times the length of parental cells (Fig. 6B), and were more frequently lysed in the absence of xylose (data not shown). The phenotype of YK207 cells (*ftsA*::*erm* P_{spac}-*ftsZ amyE*::P_{xyl}-*ylmF*), having additional xylose-inducible copy of *ylmF* at the *amyE* locus, was similar to that of parental YK206 cells when grown in the absence of xylose (Fig. 6A and B). Intriguingly, the deficiencies of growth rate and division caused by the disruption of FtsA were corrected depending on the xylose concentration in the growth medium, i.e. depending on the level of additional expression of YlmF from P_{xyl}-*ylmF* (Fig. 6A and B). In addition, a lysis of cells, which resulted in decreased growth rate, at least partly, in the *ftsA*-null strain (Jensen *et al*., 2005) was significantly suppressed by the overproduction of YlmF (data not shown). In the presence of 2% xylose, both growth rate and cell length of YK207 cells (*ftsA*::*erm* P_{spac}-*ftsZ amyE*::P_{xyl}-*ylmF*) resembled those of wild-type cells. FtsZ level were not significantly affected in YK207 cells in the absence and the presence of xylose as shown in Fig. 6D. These results demonstrated clearly that the defect in cell division caused by the *ftsA* inactivation was compensated with the YlmF overproduction. Consistent with this complementation, the reduced efficiency of Z-ring formation in the absence of FtsA was corrected by the overproduction of YlmF (Fig. 6C).

We observed anomalous, higher-order structures of FtsZ that look like spirals in the middle of cells in which YlmF is overexpressed in the absence of FtsA (Fig. 6C). Mini-cell formation at the poles was also observed. In the strain YK209 (*ftsA*::*erm* P_{spac}-*ftsZ amyE*::P_{xyl}-*ylmF aprE*::P_{ftsAZ}-*gfp-ftsZ*), an additional copy of *ftsZ* at the *aprE* locus expressed GFP-fusion proteins to approximately the same level as native proteins, as assessed by Western blotting (data not shown). However, the same amount of GFP-FtsZ did not result in the same phenotype in a wild-type, YlmF-overexpressing, or *ftsA*-null (*ftsA*::*erm* P_{spac}-*ftsZ aprE*::P_{ftsAZ}-*gfp-ftsZ*) background (data not shown). Thus, although GFP-FtsZ may contribute to mini-cell formation to a certain extent, the majority of this minor but significant phenotype is caused by the combined factors of the absence of FtsA and the overexpression of YlmF, resulting in the stabilization and/or inhibition of proper Z-ring disassembly.

Discussion

Large-scale analysis of protein complexes in *E. coli*, through the isolation of complexes using tandem affinity

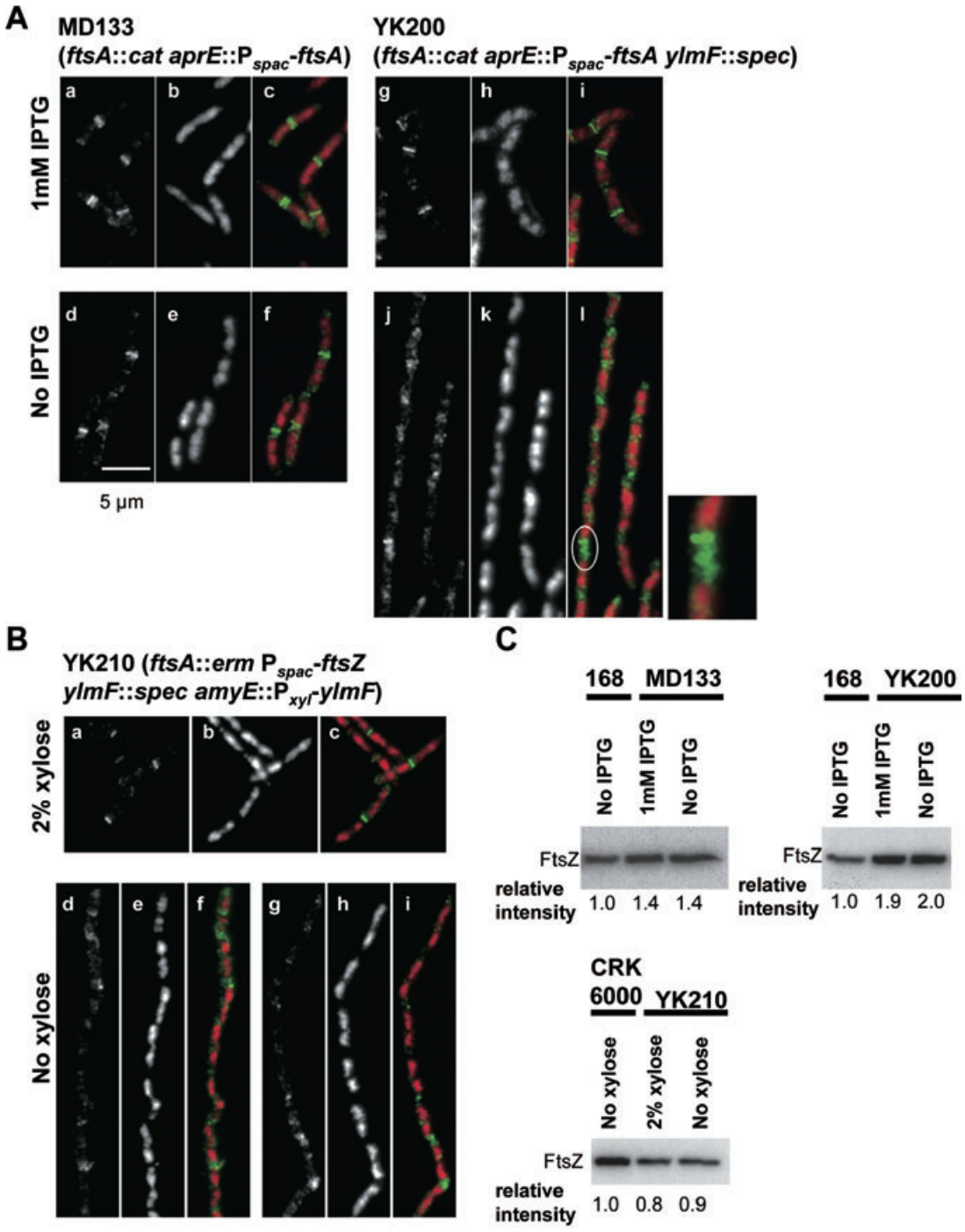

Fig. 5. Subcellular localizations of FtsZ in the double mutants of *ftsA* and *ylmF*.
A. Immunolocalization of FtsZ in MD133 (*ftsA*::*cat aprE*::P_{spac}-*ftsA*; a–f) and YK200 (*ftsA*::*cat aprE*::P_{spac}-*ftsA ylmF*::*spec*; g–l) cells. The panels show Cy2 immunofluorescence (a, d, g and j), DAPI (b, e, h and k) and merged images (c, f, i and l), indicating Cy2 immunofluorescence in green and DAPI in red. MD133 cells and YK200 were collected for analysis at 0 (1 mM IPTG: a–c and g–i) and 90 min (no IPTG: d–f and j–l) after the removal of xylose from medium. Enlarged image of an example of a spiral-like structure, indicated by circle, is included.
B. Immunolocalization of FtsZ in YK210 cells (*ftsA*::*erm* P_{spac}-*ftsZ ylmF*::*spec amyE*::P_{xyl}-*ylmF*). The panels show Cy2 immunofluorescence (a, d and g), DAPI (b, e and h) and merged images (c, f and i), with Cy2 immunofluorescence in green and DAPI in red. YK210 cells were collected for analysis at 0 (a–c) and 90 min [d–i; two sets of images (d–f and g–l) of different fields in the same preparations are shown] after the removal of xylose from medium.
C. FtsZ levels in MD133, YK200 and YK210 cells, and their parental wild-type cells, 168 and CRK6000, were analysed by Western blotting using anti-FtsZ serum. Each strain was cultured in the same conditions as described in panels A or B, and total cellular proteins from equal amount of cells were analysed.

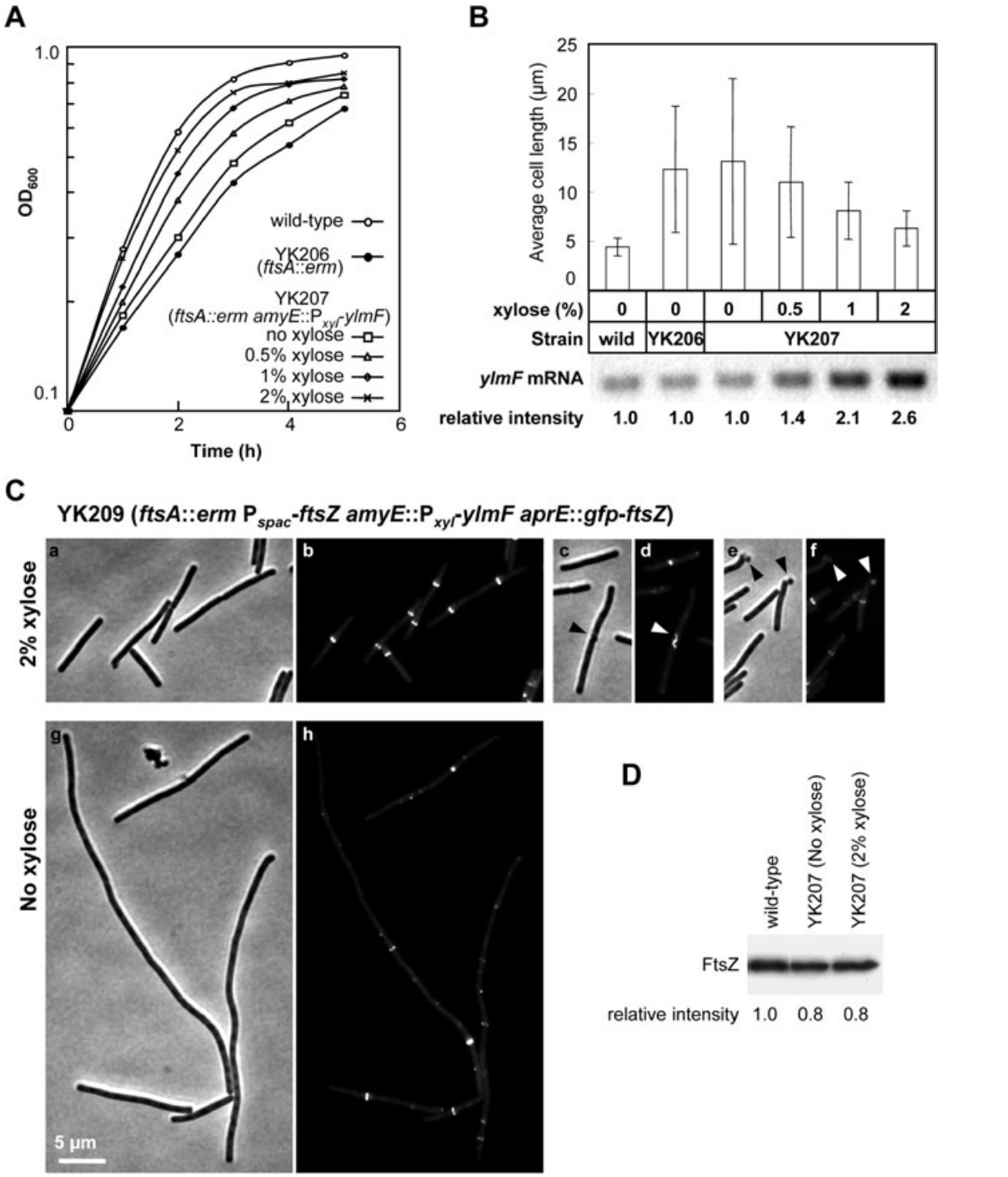

Fig. 6. Effects of YlmF overexpression on the *ftsA*-null phenotype.
A. Growth of YK207 cells (*ftsA*::*erm* P_{spac}-*ftsZ amyE*::P_{xyl}-*ylmF*) in PAB medium in the presence of various xylose concentrations at 30°C is shown. Growth of CRK6000 (wild-type) and YK206 (*ftsA*::*erm* P_{spac}-*ftsZ*) cells in PAB medium are also shown as controls.
B. Average length of 500 cells for each strain at exponential growth phase (OD_{600} = 0.3) is indicated by error bars. Expression levels of the *ylmF* mRNA were measured by quantitative RT-PCR as described in *Experimental procedures* and gel images of RT-PCR products in each condition are shown in the bottom.
C. Phase-contrast (a, c, e and g) and GFP-FtsZ (b, d, f and h) images of exponential phase YK209 cells (*ftsA*::*erm* P_{spac}-*ftsZ amyE*::P_{xyl}-*ylmF aprE*::*gfp-ftsZ*) grown in the presence (a–f) and absence (g and h) of 2% xylose, which induces YlmF. ab, cd and ef were different fields of the same preparation. Mini-cells and FtsZ-spirals are depicted by arrowheads.
D. FtsZ levels in CRK6000 (wild-type) cells cultured in PAB medium and YK207 (*ftsA*::*erm* P_{spac}-*ftsZ amyE*::P_{xyl}-*ylmF*) cells grown in PAB medium in the absence and presence of 2% xylose were analysed by Western blotting using anti-FtsZ serum. Total cellular proteins from equal amount of cells were analysed.

purification or sequential peptide affinity tags followed by mass spectrometry, has allowed the identification of many protein–protein interactions but has failed to detect the known interaction between FtsZ and FtsA. This failure may be because detectable interactions have been limited to the identification of relatively stable complexes (Butland *et al*., 2005). In the present study, in order to prevent the dissociation of *in vivo* complexes during purification, we applied a cross-linking method and successfully demonstrated that EzrA and ZapA are indeed involved in a protein complex with FtsZ *in vivo*, as well as with FtsA, whose *in vivo* interaction with FtsZ was previously described (Jensen *et al*., 2005). More importantly, we identified YlmF as a new component of the FtsZ complex. Thus, the procedure presented here not only provided important clues to understand the mechanism of Z-ring formation but also provides a useful strategy for finding new factors present in unstable complexes.

Functional analysis of the *B. subtilis* YlmF protein in this study demonstrated that YlmF is indeed one of the cell division proteins that localizes to sites of cell division probably through its direct interaction with FtsZ. Furthermore, we demonstrated synthetic lethality after simultaneous depletion of both YlmF and FtsA due to complete inhibition of Z-ring formation and thus cell division, and the complementation of a *ftsA*-null phenotype by the overexpression of YlmF. Comparative analysis of complete, available, bacterial genome sequences using the Microbial Genome Database (Uchiyama, 2003) showed that YlmF is conserved in Firmicutes (i.e. low G+C content, Gram-positive bacteria, including *B. subtilis*), Symbiobacteria, Fusobacteria, Actinobacteria (i.e. high G+C content, Gram-positive bacteria), and Cyanobacteria. On the other hand, FtsA is conserved in Firmicutes, Symbiobacteria, Proteobacteria and some additional phyla. Mollicutes, commonly called mycoplasmas in a class of Firmicutes, is exceptional as some of them lack even FtsZ as well as FtsA and/or YlmF. Interestingly, YlmF was recently shown to be an essential gene in the Cyanobacterium, *S. elongatus* PCC 7942 (Miyagishima *et al*., 2005), which lacks FtsA. Conversely, FtsA is an essential gene in both *E. coli* and *Caulobacter crescentus* (Lutkenhaus and Donachie, 1979; Sackett *et al*., 1998), Proteobacteria that lack YlmF. These results are consistent with our finding that both FtsA and YlmF have overlapping roles in *B. subtilis* cell division and that expression of either protein is essential for *B. subtilis* cell division and growth. Thus, it also suggested that YlmF would play a critical role in cell division in FtsA-lacking bacteria, as FtsA does in YlmF-lacking bacteria, and that both FtsA and YlmF would work additively with FtsZ in bacteria that possess both proteins. In *B. subtilis*, the disruption of *ylmF* partially impairs cell division without affecting growth rate. Meanwhile, the *ftsA*-null mutation causes a severe defect in cell division, suggesting that FtsA contributes more strongly to cell division than does YlmF. Although unexpected, it has been reported that disruption of *ylmF* caused a partial cell division defect in affected strains (Fadda *et al*., 2003) but *ftsA* remained an essential gene in *S. pneumoniae* (Lara *et al*., 2005). However, the absolute requirement for FtsA was determined by its unsuccessful gene replacement within the *cat* cassette by a double-crossing over event (Lara *et al*., 2005). As *ftsA* is present in an operon with *ftsZ* in *S. pneumoniae*, we speculated that the replacement of *ftsA* with *cat* would result in a synthetic lethal effect, both because of the absence of FtsA and the consequently changed expression levels of FtsZ. This effect was in fact observed in *B. subtilis* when *ftsA*::*cat* from MD133 (*ftsA*::*cat aprE*::P_{spac}-*ftsA*) was introduced into wild-type cells.

In *E. coli*, ZipA was shown to have overlapping functions with FtsA for the formation and/or stabilization of the Z ring, similar to the role for YlmF in *B. subtilis* reported here, although both FtsA and ZipA are essential for *E. coli* growth. In spite of the similar functions of FtsA, ZipA and YlmF, their masses (molecular weights of YlmF, ZipA and FtsA are 17, 37 and 48 kDa respectively) and overall amino acid sequences are quite different. How then can such different proteins promote Z-ring formation? The cross-linking of FtsZ protofilaments by ZapA dimer or tetramer bridges has been proposed as a possible mechanism based on *in vitro* studies (Gueiros-Filho and Losick, 2002; Low *et al*., 2004). As for FtsA, a proposed mechanism has not yet been directly demonstrated, but evidence in *E. coli* suggests that destabilization of either FtsA–FtsZ or FtsA–FtsA interactions results in severe defects in cell division (Ma and Margolin, 1999; Yim *et al*., 2000; Rico *et al*., 2004). In agreement with these observations, we found that YlmF interacted with both FtsZ and itself. Thus, YlmF may also be able to promote Z-ring formation by cross-linking FtsZ protofilaments.

The highly conserved C-terminal region of FtsZ has been determined to be essential for interactions with both FtsA and ZipA but not for localization or multimerization of FtsZ at sites of cell division (Wang *et al*., 1997; Ma and Margolin, 1999). Furthermore, the crystal structure of the ZipA–FtsZ C-terminal peptide (amino acids 367–383) complex was solved and showed that Ile374, Phe377 and Leu378 were all important amino acids for binding. This complex forms by hydrophobic contacts that are independent of amino acid side-chain specificity, implying that there are less steric constraints on binding partners (Mosyak *et al*., 2000). Interestingly, this FtsZ peptide is highly conserved in both Actinobacteria and Cyanobacteria, which have no FtsA homologue. Thus, these facts suggest that this peptide may be responsible for binding to YlmF in certain bacteria, including *B. subtilis*.

It should be noted that when YlmF was overexpressed in a *ftsA*-null background, not only was the reduced effi-

ciency of Z-ring formation corrected but cell division also recovered to normal levels, indicating that an excess amount of YlmF could compensate for both the recruitment of cell division proteins during later stages of cell division and the constriction of Z rings. Thus, our results may suggest that some structure in the Z ring promoted by FtsA and/or YlmF recruits downstream cell division proteins, but that neither FtsA nor YlmF recruit them through direct interaction. On the other hand, FtsA has been shown to be essential for the recruitment of downstream cell division proteins; there are evidences for a direct interaction of FtsA with FtsI in *E. coli* (Di Lallo *et al*., 2003; Corbin *et al*., 2004; Karimova *et al*., 2005). Thus, it is possible that *B. subtilis* FtsA interacts with PbpB, counterpart of *E. coli* FtsI, and if so, this might explain how FtsA contributes more strongly to cell division than does YlmF. Although interactions between FtsA and downstream proteins including PbpB could not be specifically detected in our study, this fact does not preclude the presence of direct interactions because purification of membrane-spanning proteins and detection of small proteins by mass spectrometry would be technically difficult. It is also possible that the use of FtsA-His, which is not fully functional in cell division, may be the reason why the downstream cell division proteins could not be detected in the complex.

During preparing this manuscript, Hamoen *et al*. (2005) reported that YlmF (SepF) acts in cell division. They showed that YlmF binds to FtsZ and itself, YlmF localizes to division sites depending on FtsZ, and the disruption results in partial defect in cell division, as reported in this study. They further demonstrated that combination of a *ylmF* and *ezrA* mutation resulted in a synthetic-lethal division defect, although Z rings and a late assembling division protein, Pbp2B, still assembled in the filamentous cells. Therefore, Hamoen *et al*. proposed that YlmF is not involved in Z-ring formation and divisome assembly, but is active in a later step of cell division process; the constriction of the divisome and/or synthesis of the septum wall. However, similar synergistic effect has been reported when EzrA and ZapA are simultaneously underexpressed, even though ZapA acts in an early step of cell division by promoting the assembly of FtsZ (Gueiros-Filho and Losick, 2002). Moreover, we recently reported that expression of YneA, which suppresses cell division during the SOS response, and disruption of *noc*, which acts as an effector of nucleoid occlusion, in *ezrA* mutant cells resulted in accumulation of multiple non-constricting Z rings and lethal division defect (Kawai and Ogasawara, 2006). EzrA has been proposed as a negative regulator of Z-ring formation, and the inactivation stabilizes Z ring and it leads to the limiting amount of FtsL (Levin *et al*., 2001; Kawai and Ogasawara, 2006), which is essential for the complete assembly of late division complex and the following constriction process (Daniel *et al*., 1998). Interestingly, FtsL overproduction could suppress the synthetic defect caused by the expression of YneA and disruption of *noc* or *zapA* in *ezrA*$^-$ background (Kawai and Ogasawara, 2006). The synthetic lethality of simultaneous deletion of *ylmF* and *ezrA* was also suppressed by the FtsL overproduction (data not shown).

As demonstrated in this study, *B. subtilis* contains two proteins, FtsA and YlmF, which differ in both size and homology but can independently promote the same early-stage processes in cell division. At this point, *B. subtilis* is a unique bacterial model that will be useful for further studies of bacterial cytokinesis. Additional functional analyses of both proteins will provide a better understanding of early-stage cytokinetic events.

Experimental procedures

Bacterial strains and cell growth

The *B. subtilis* strains used in this study are listed in Table 1. *B. subtilis* 168, CRK6000, and their derivatives were grown in either LB medium or antibiotic medium 3 (PAB; Difco Laboratories), supplemented with adenine and guanosine (20 μg ml^{-1} each) at 37°C, unless otherwise stated. When appropriate, erythromycin, chloramphenicol, tetracycline and spectinomycin were added to the medium at final concentrations of 0.5, 5, 10 and 100 μg ml^{-1} respectively. The *E. coli* strains DH5α, C600, and XL10-Gold (Stratagene) were used for plasmid construction and propagation.

Plasmid construction

All primers used for PCR are listed in Table S1. Structures of plasmids and strains constructed in this study were examined by DNA sequencing to avoid PCR mutations.

The pMUTinHis plasmid was employed in the fusion of a histidine tag to the 3′-terminus of target genes. Fragment that encoded 12 histidines with cloning sites at both ends was amplified by PCR using 2HC-F and 2H-3Stop primers from pSI2HC (S. Ishikawa and N. Ogasawara, unpublished) and then inserted between the SalI and SacI sites of pMutinNC (Morimoto *et al*., 2002). To construct pMUTinHis-ΔftsA, -ΔftsZ, -ΔzapA, -ΔezrA, -ΔylmF and -ΔdnaC, 260–500 bp fragments, encoding the 3′ portion of each gene except for the stop codon, were amplified by PCR using the following primer sets: ftsA.f–ftsA.r, ftsZ.f–ftsZ.r, zapA.f–zapA.r, ezrA.f–ezrA.r, ylmF.f–ylmF.r and dnaC.f–dnaC.r, respectively, from *B. subtilis* 168 genomic DNA and were subsequently cloned in the HindIII or EcoRI and XhoI sites of pMUTinHis.

Plasmid manipulation of the *B. subtilis* genes was accomplished using the Gateway cloning technology, as per the manufacturer's instructions (Invitrogen). The coding sequences were amplified from the wild-type 168 chromosome by PCR using primers containing the *attB* sequence at both ends and were cloned into the pDONR201 plasmid by BP clonase to create entry clones. Entry clones were used to construct expression clones through recombination reactions between the entry clone and the destination vector.

Table 1. *B. subtilis* strains and mutants used in this study.

Strain	Relevant genotype[a]	Source or reference[b]
168	*trpC2*	Pasteur stock (Vagner *et al*., 1998)
168ftsAHis	168 *ftsA*::pMUTinHisΔftsA	pMUTinHisΔftsA → 168
168ftsZHis	168 *ftsZ*::pMUTinHisΔftsZ	pMUTinHisΔftsZ → 168
168zapAHis	168 *zapA*::pMUTinHisΔzapA	pMUTinHisΔzapA → 168
168ezrAHis	168 *ezrA*::pMUTinHisΔezrA	pMUTinHisΔezrA → 168
168ylmFHis	168 *ylmF*::pMUTinHisΔylmF	pMUTinHisΔylmF → 168
168dnaCHis	168 *dnaC*::pMUTinHisΔdnaC	pMUTinHisΔdnaC → 168
ASK600	168 *aprE*::P_{ftsAZ}-*gfp-ftsZ (spec*)	Kei Asai (unpublished)
ts1	168 *ts1*(*ftsZ1*)	Callister *et al*. (1983)
YK199	168 *ts1*(*ftsZ1*) *aprE*::P_{spac}-*yfp-ylmF (spec*)	YK203 → ts1
MD133	168 *ftsA*::*cat aprE*::P_{spac}-*ftsA (kan*)	M. Yoshimura and N. Ogasawara (unpublished)
YK200	168 *ftsA*::*cat aprE*::P_{spac}-*ftsA (kan*) *ylmF*::*spec*	YK204 → MD133
YK201	168 *ftsA*::*cat aprE*::P_{spac}-*ftsA (kan*) *ezrA*::*spec*	YK012 → MD133
YK202	168 *ftsA*::*cat aprE*:: P_{spac}-*ftsA* (*kan*) *zapA*::*spec*	YK013 → MD133
CRK6000	*purA16 metB5 hisA3 guaB*	Laboratory stock (Moriya *et al*., 1990)
YK012	CRK6000*ezrA*::*spec*	Kawai and Ogasawara (2006)
YK013	CRK6000*zapA*::*spec*	Kawai and Ogasawara (2006)
YK203	CRK6000*aprE*::P_{spac}-*yfp-ylmF*(*spec*)	pAPNC213-yfp-ylmF → CRK6000
YK204	CRK6000*ylmF*::*spec*	PCR product → CRK6000
YK205	CRK6000*ylmF*::*spec amyE*::P_{xyl}-*ylmF (tet*)	pXTylmF → YK204
YK206	CRK6000*ftsA*::*erm* P_{spac}-*ftsZ*	PCR product → CRK6000
YK207	CRK6000*ftsA*::*erm* P_{spac}-*ftsZ amyE*::P_{xyl}-*ylmF (tet*)	pXTylmF → YK206
YK208	CRK6000*aprE*::P_{ftsAZ}-*gfp-ftsZ (spec*)	ASK600 → CRK6000
YK209	CRK6000*ftsA*::*erm* P_{spac}-*ftsZ amyE*::P_{xyl}-*ylmF (tet*) *aprE*::P_{ftsAZ}-*gfp-ftsZ* (*spec*)	ASK600 → YK207
YK210	CRK6000*ftsA*::*erm* P_{spac}-*ftsZ amyE*::P_{xyl}-*ylmF (tet*) *ylmF*::*spec*	YK204 → YK207

a. Antibiotic resistance genes are expressed as follows: *cat,* chloramphenicol; *kan,* kanamycin; *spec,* spectinomycin; *tet,* tetracycline; *emr,* erythromycin.
b. Arrows indicate construction by transformation using plasmid DNA, chromosomal DNA, or PCR products.

To attach either the entire *attB*1 or *attB*2 sequence at either end of the PCR product, we used two-step adaptor PCR. For the first step, PCR was performed for six cycles using specific forward and reverse primers that contained half the sequence of *attB*1 (5′-AAAAAGCAGGCTCG-3′) or *attB*2 (5′-AGAAAGCTGGGTC-3′) at the 5′ end respectively. Then, the first reaction mixture was used as a template for the second reaction using adaptor-attB1 and adaptor-attB2 primers that contained the entire *attB*1 and *attB*2 sequences respectively. In this study, *ftsA*, *ftsZ*, *zapA*, *ezrA* and *ylmF* sequences were amplified using the following primer sets: ftsAgwF–ftsAgwR, ftsZgwF–ftsZgwR, zapAgwF–zapAgwR, ezrAgwF–ezrAgwR and ylmFgwF–ylmFgwR respectively, and were subsequently cloned into pDONR201 (Invitrogen) to create entry clones (i.e. pENTR-ftsA, -ftsZ, -zapA, -ezrA and -ylmF).

The pGBT9 and pGAD424 plasmids for yeast two-hybrid experiments were obtained from Clontech. To convert these plasmids to Gateway system destination vectors, pGBT9 and pGAD424 were doubly digested with EcoRI and BamHI, Mung Bean nuclease was added to create blunt ends (Takara Bio), and the plasmids were ligated into the rfC cassette (Invitrogen). The resulting destination vectors were designated pDBGW and pADGW respectively. The pGBT9 derivatives (i.e. pGBT9-ftsA, -ftsZ, -zapA, -ezrA and -ylmF) and the pGAD424 derivatives (i.e. pGAD424-ftsA, -ftsZ, -zapA, -ezrA and -ylmF) were constructed by recombination reactions between the entry clones (i.e. pENTR-ftsA, -ftsZ, -zapA, -ezrA and -ylmF) and the destination vectors, pDBGW and pADGW.

To construct the destination vector for the integration of the IPTG-regulated *yfp*-fusion gene at the *aprE* locus on the *B. subtilis* chromosome, the *yfp* gene was amplified from pMyfp (Lindow *et al*., 2002) using primers fp-SD-HBg-F and fp-rfA-R [fp-rfA-R has a region that is homologous to the *attR*1 sequence of the rfA cassette (Invitrogen) at its 5′ end]. The *yfp*-rfA fragment was created by recombinant PCR using both the amplified *yfp* fragment and the rfA cassette as templates, and using primers fp-HBg-F and attR2-EVBg-R (anneals to the *attR*2 sequence). The resulting PCR product was digested with BglII and EcoRV and subsequently cloned into the BamHI and SmaI sites of pAPNC213 (Morimoto *et al*., 2002). The resulting destination vector was designated pAPNC213-yfp-GW. The plasmid pAPNC213-yfp-ylmF was constructed by a recombination reaction between pENTR-ylmF and pAPNC213-yfp-GW. To construct pXT, the *tet* cassette, which was amplified from pBEST307 (Itaya, 1992) using the tetF2-tetR2 primer set (Kawai *et al*., 2003), was cloned into the EcoRV site of pX, an integration vector, into the *amyE* locus for xylose-inducible gene expression (Kim *et al*., 1996). The *ylmF* fragment, containing both its ribosome binding site and stop codon, was amplified using SDylmF-SpeI and ylmF-BR primers, digested with SpeI and BglII, and cloned into the SpeI and BamHI sites in pXT. The resulting plasmid (pXTylmF) was integrated into the *amyE* locus of the *B. subtilis* chromosome by two crossing-over events to create a mutant in which *ylmF* expression could be induced by xylose.

Construction of strains expressing histidine-tagged fusions

Bacillus subtilis strains that had histidine tags fused to the 3′

end of each gene on the chromosome was constructed by integrating the pMUTinHis derivatives (Fig. 1A and Table 1). Strain 168ftsZHis grew normally, but 168ftsAHis cells become elongated, in the presence of 1 mM IPTG to ensure downstream *ftsZ* expression, although growth rate was not affected, indicating that FtsA-His was not fully functional. Growth rate of 168ezrAHis and 168zapAHis was also normal. In addition, null mutation of *ezrA* (*ezrA*::*spec*) could be introduced into strain 168zapAHis and *zapA::spec* into 168ezrAHis, although *ezrA zapA* double disruption resulted in synthetic defect in cell division (Gueiros-Filho and Losick, 2002), indicating that the both fusions were functional. Synthetic lethality of the simultaneous deletion of *ylmF* and *ezrA* has also been reported (Hamoen *et al*., 2005) and null mutation of *ezrA (ezrA*::*spec*) could not be introduced into strain 168ylmFHis, suggesting that YlmF-His was not fully functional, although growth rate of 168ylmFHis cells was normal.

Construction of ylmF *and* ftsA *deletion mutants*

To construct the *ylmF* deletion mutant, the 5′ upstream and 3′ downstream regions of *ylmF* were amplified from *B. subtilis* 168 chromosomal DNA using primer sets ylmDHF–ylmFdel1R (complementary rPCR1 sequence, GGATA GACTCCACCAGAAGAGC, at its 3′ end) and ylmFdel2F (with the rPCR2 sequence, CGGAAGGATACTACATCCTGG, at its 3′ end)–ylmHXR respectively. The *spec* gene with the promoter region was amplified from pJL62 (LeDeaux and Grossman, 1995) using rPCR–SpecF2 (with the rPCR1 sequence at its 3′ end) and rPCR–SpecR2 (complementary rPCR2 sequence at its 3′ end). The resulting three fragments were joined by recombinant PCR using the ylmDHF–ylmHXR primer set and integrated into the *B. subtilis* chromosome by two crossing-over events.

To construct the *ftsA*-null mutant, the upstream and downstream regions of *ftsA* were amplified from *B. subtilis* 168 chromosomal DNA using primer sets fAd1F–fAd1R and fAd2F–fAd2R respectively, and a 1.9 kb sequence, containing both the *erm* gene and P_{spac}, was amplified from pMutinNC (Morimoto *et al*., 2002) using spacFS (complementary fAd1R sequence at its 5′ end) and spacR (complementary fAd2F sequence at its 5′ end). The resulting three fragments were joined by recombinant PCR using the fAd1F–fAd2R primer set and integrated into the *B. subtilis* chromosome by two crossing-over events.

Purification of protein complexes

An overnight liquid culture of *B. subtilis* cells expressing histidine-tagged protein in LB medium containing 0.5 μg ml^{-1} erythromycin and 1 mM IPTG at 30°C was inoculated into 200 ml of the same medium at an initial OD_{600} of 0.01. When the cells, grown at 37°C, reached an OD_{600} of 0.5–0.6, the culture was treated with formaldehyde (0.4% final concentration) for 30 min. Tris-HCl (2 M, pH 9.0) was added at a final concentration of 20 mM and the culture was incubated for an additional 10 min. Cells were washed twice with 20 mM Tris-HCl (pH 7.5) and stored at −80°C. Collected cells were disrupted by sonication on ice in U buffer (100 mM Hepes, 50 mM imidazole, 8 M urea, 0.5 M NaCl, 1 mM DTT and 1 mM PMSF, pH 7.4). After centrifugation at 8000 rpm for 10 min, MagneHis beads (Promega) were added to the supernatant, followed by incubation at room temperature for 2 h with gentle shaking. MagneHis beads were washed three times with U buffer and bound proteins were eluted with elution buffer [100 mM Tris-HCl (pH 7.5), 0.5 M imidazole, 1% SDS, and 1 mM DTT]. To remove non-specifically bound, uncross-linked proteins, the eluate was passed through a Microcon-100 column (Millipore) to remove proteins with molecular masses lower than 100 kDa. Protein complexes that were retained on the membrane were washed twice with elution buffer and recovered by addition of 20 μl of the same buffer. Cross-linked proteins were dissociated by heating overnight at 65°C. To identify proteins in the complex by mass spectrometry, eluates were separated by SDS-PAGE after heating; separated proteins were visualized by Coomassie brilliant blue R-250 staining. In-gel enzymatic digestion, peptide analysis, and protein identification by LC-MS/MS were carried out as described by Kuwana *et al*. (2002).

Fluorescence microscopy

Live cells were examined on agarose slides (Price and Losick, 1999). Cell morphology and nucleoid distribution were examined by fluorescence microscopy after DAPI (4′,6-diamino-2phenyl indole) staining, as described previously (Hassan *et al*., 1997). Fluorescence was detected using fluorescence microscopy (DMRE-HC, Leica), a cooled digital CCD camera (1300Y, Roper Scientific), and a YFP filter set (Omega). Images were uploaded and analysed to determine the intracellular locations of the signals using MetaMorph software (Universal Imaging). Immunofluorescence microscopy was performed as by Kawai *et al*. (2003).

Yeast two-hybrid analysis

Yeast strains, PJ69-4 A (*MAT*a, *trp1-901*, *leu2-3*, *112ura3-52*, *his-200*, *gal4*Δ, *gal80*Δ, *LYS2*::*GAL1-HIS3*, *GAL2-ADE2*, *met2*::*GAL7-lacZ*) and PJ69-4α (*MAT*α, *trp1-901*, *leu2-3*, *112ura3-52*, *his-200*, *gal4*Δ, *gal80*Δ, *LYS2*::*GAL1-HIS3*, *GAL2-ADE2*, *met2*::*GAL7-lacZ*) were kindly provided by Philip James (James *et al*., 1996).

The pGBT9 derivative (*TRP1*) and the pGAD424 derivative (*LEU2*) were used to transform PJ69-4A and PJ69-4α respectively, using the method described by Bongiorni *et al*. (2005) with minor modifications. Transformants were mated in the appropriate liquid medium using flat-bottomed, 96 well plates. After mating, the cultures were collected, washed with sterilized water, and spotted onto synthetic complete (SC) agar plates that lacked leucine and tryptophan (SC-LW) for selection of *LEU2* and *TRP1* diploid cells. Selected cells were cultured in liquid SC-LW for 1 day and were then replica-plated on selection agar medium that lacked histidine (SC-LEH) and contained 5 mM 3-aminotrizaole (3-AT) to inhibit auto-activation of the *HIS3*-reporter gene.

Quantitative RT-PCR

Total cellular RNA was extracted from *B. subtilis* cells as described previously (Kawai *et al*., 2003). First-strand cDNA was synthesized from 15 μg of RNA using the SuperScript III

reverse transcriptase and random primers following the manufacturer's instructions (Invitrogen). In the second PCR reaction, a 108 bp internal sequence of *ylmF* was amplified by iProof High-Fidelity DNA polymerase (BIO-RAD) using ylmFmeasureF and ylmFmeasureR primers, which were designed by Primer3 software (Rozen and Skaletsky, 2000). Various concentrations of the cDNA products were used as templates to determine the appropriate condition for quantitative amplification. After the optimization, quantitative RT-PCR was performed 30 cycles using 2 μl of 3.2×10^4 times diluted first cDNA reaction mixture as template in 20 μl of total volume, and then 5 μl of the products was separated in a 2% agarose gel, followed by ethidium bromide staining. Gel images were photographed on a UV illuminator and the amount of DNA was quantified by NIH Image (http://rsb.info.nih.gov/nih-image/).

Western blotting

Western blotting was performed following the instructions of ECL Plus Western blotting detection system (Amersham). The details are described in *Supplementary material*.

Acknowledgements

We thank Mika Yoshimura and Kei Asai for generous gifts of mutant strains, Taku Oshima for valuable discussions. This work was supported by a Grant-in-Aid for Scientific Research on Priority Areas, Life System Informatics, from the Ministry of Education, Culture, Sports, Science and Technology of Japan.

References

Aarsman, M.E., Piette, A., Fraipont, C., Vinkenvleugel, T.M., Nguyen-Disteche, M., and den Blaauwen, T. (2005) Maturation of the *Escherichia coli* divisome occurs in two steps. *Mol Microbiol* **55:** 1631–1645.

Beall, B., and Lutkenhaus, J. (1992) Impaired cell division and sporulation of a *Bacillus subtilis* strain with the *ftsA* gene deleted. *J Bacteriol* **174:** 2398–2403.

Bongiorni, C., Ishikawa, S., Stephenson, S., Ogasawara, N., and Perego, M. (2005) Synergistic regulation of competence development in *Bacillus subtilis* by two Rap-Phr systems. *J Bacteriol* **187:** 4353–4361.

Bruand, C., Farache, M., McGovern, S., Ehrlich, S.D., and Polard, P. (2001) DnaB, DnaD and DnaI proteins are components of the *Bacillus subtilis* replication restart primosome. *Mol Microbiol* **42:** 245–255.

Butland, G., Peregrin-Alvarez, J.M., Li, J., Yang, W., Yang, X., Canadien, V., *et al.* (2005) Interaction network containing conserved and essential protein complexes in *Escherichia coli*. *Nature* **433:** 531–537.

Callister, H., McGinness, T., and Wake, R.G. (1983) Timing and other features of the action of the ts1 division initiation gene product of *Bacillus subtilis*. *J Bacteriol* **154:** 537–546.

Cha, J.H., and Stewart, G.C. (1997) The *divIVA* minicell locus of *Bacillus subtilis*. *J Bacteriol* **179:** 1671–1683.

Corbin, B.D., Geissler, B., Sadasivam, M., and Margolin, W. (2004) Z-ring-independent interaction between a subdomain of FtsA and late septation proteins as revealed by a polar recruitment assay. *J Bacteriol* **186:** 7736–7744.

Daniel, R.A., and Errington, J. (2003) Control of cell morphogenesis in bacteria: two distinct ways to make a rod-shaped cell. *Cell* **113:** 767–776.

Daniel, R.A., Harry, E.J., Katis, V.L., Wake, R.G., and Errington, J. (1998) Characterization of the essential cell division gene *ftsL* (*yIID*) of *Bacillus subtilis* and its role in the assembly of the division apparatus. *Mol Microbiol* **29:** 593–604.

Di Lallo, G., Fagioli, M., Barionovi, D., Ghelardini, P., and Paolozzi, L. (2003) Use of a two-hybrid assay to study the assembly of a complex multicomponent protein machinery: bacterial septosome differentiation. *Microbiology* **149:** 3353–3359.

Edwards, D.H., and Errington, J. (1997) The *Bacillus subtilis* DivIVA protein targets to the division septum and controls the site specificity of cell division. *Mol Microbiol* **24:** 905–915.

Errington, J., Daniel, R.A., and Scheffers, D.J. (2003) Cytokinesis in bacteria. *Microbiol Mol Biol Rev* **67:** 52–65.

Fadda, D., Pischedda, C., Caldara, F., Whalen, M.B., Anderluzzi, D., Domenici, E., and Massidda, O. (2003) Characterization of *divIVA* and other genes located in the chromosomal region downstream of the *dcw* cluster in *Streptococcus pneumoniae*. *J Bacteriol* **185:** 6209–6214.

Feucht, A., Lucet, I., Yudkin, M.D., and Errington, J. (2001) Cytological and biochemical characterization of the FtsA cell division protein of *Bacillus subtilis*. *Mol Microbiol* **40:** 115–125.

Geissler, B., Elraheb, D., and Margolin, W. (2003) A gain-of-function mutation in *ftsA* bypasses the requirement for the essential cell division gene *zipA* in *Escherichia coli*. *Proc Natl Acad Sci USA* **100:** 4197–4202.

Gueiros-Filho, F.J., and Losick, R. (2002) A widely conserved bacterial cell division protein that promotes assembly of the tubulin-like protein FtsZ. *Genes Dev* **16:** 2544–2556.

Haeusser, D.P., Schwartz, R.L., Smith, A.M., Oates, M.E., and Levin, P.A. (2004) EzrA prevents aberrant cell division by modulating assembly of the cytoskeletal protein FtsZ. *Mol Microbiol* **52:** 801–814.

Hale, C.A., and de Boer, P.A. (1997) Direct binding of FtsZ to ZipA, an essential component of the septal ring structure that mediates cell division in *E. coli*. *Cell* **88:** 175–185.

Hamoen, L.W., Meile, J.-C., de Jong, W., Noirot, P., and Errington, J. (2005) SepF, a novel FtsZ-interacting protein required for a late step in cell division. *Mol Microbiol* **59:** 989–999.

Hassan, A.K., Moriya, S., Ogura, M., Tanaka, T., Kawamura, F., and Ogasawara, N. (1997) Suppression of initiation defects of chromosome replication in *Bacillus subtilis dnaA* and *oriC*-deleted mutants by integration of a plasmid replicon into the chromosomes. *J Bacteriol* **179:** 2494–2502.

Imai, Y., Ogasawara, N., Ishigo-Oka, D., Kadoya, R., Daito, T., and Moriya, S. (2000) Subcellular localization of Dna-initiation proteins of *Bacillus subtilis*: evidence that chromosome replication begins at either edge of the nucleoids. *Mol Microbiol* **36:** 1037–1048.

Itaya, M. (1992) Construction of a novel tetracycline resistance gene cassette useful as a marker on the *Bacillus*

subtilis chromosome. *Biosci Biotechnol Biochem* **56:** 685–686.

James, P., Halladay, J., and Craig, E.A. (1996) Genomic libraries and a host strain designed for highly efficient two-hybrid selection in yeast. *Genetics* **144:** 1425–1436.

Jensen, S.O., Thompson, L.S., and Harry, E.J. (2005) Cell division in *Bacillus subtilis*: FtsZ and FtsA association is Z-ring independent, and FtsA is required for efficient midcell Z-Ring assembly. *J Bacteriol* **187:** 6536–6544.

Jones, L.J.F., Carballido-Lopez, R., and Errington, J. (2001) Control of cell shape in bacteria: helical, actin-like filaments in *Bacillus subtilis*. *Cell* **104:** 913–922.

Karimova, G., Dautin, N., and Ladant, D. (2005) Interaction network among *Escherichia coli* membrane proteins involved in cell division as revealed by bacterial two-hybrid analysis. *J Bacteriol* **187:** 2233–2243.

Kawai, Y., and Ogasawara, N. (2006) *Bacillus subtilis* EzrA and FtsL synergistically regulate FtsZ ring dynamics during cell division. *Microbiology* **152:** 1129–1141.

Kawai, Y., Moriya, S., and Ogasawara, N. (2003) Identification of a protein, YneA, responsible for cell division suppression during the SOS response in *Bacillus subtilis*. *Mol Microbiol* **47:** 1113–1122.

Kim, L., Mogk, A., and Schumann, W. (1996) A xylose-inducible *Bacillus subtilis* integration vector and its application. *Gene* **181:** 71–76.

Kuwana, R., Kasahara, Y., Fujibayashi, M., Takamatsu, H., Ogasawara, N., and Watabe, K. (2002) Proteomics characterization of novel spore proteins of *Bacillus subtilis*. *Microbiology* **148:** 3971–3682.

Lara, B., Rico, A.I., Petruzzelli, S., Santona, A., Dumas, J., Biton, J., *et al.* (2005) Cell division in cocci: localization and properties of the *Streptococcus pneumoniae* FtsA protein. *Mol Microbiol* **55:** 699–711.

Layh-Schmitt, G., Podtelejnikov, A., and Mann, M. (2000) Proteins complexed to the P1 adhesin of *Mycoplasma pneumoniae*. *Microbiology* **146:** 741–747.

LeDeaux, J.R., and Grossman, A.D. (1995) Isolation and characterization of *kinC*, a gene that encodes a sensor kinase homologous to the sporulation sensor kinases KinA and KinB in *Bacillus subtilis*. *J Bacteriol* **177:** 166–175.

Levin, P.A., Kurtser, I.G., and Grossman, A.D. (1999) Identification and characterization of a negative regulator of FtsZ ring formation in *Bacillus subtilis*. *Proc Natl Acad Sci USA* **96:** 9642–9647.

Levin, P.A., Schwartz, R.L., and Grossman, A.D. (2001) Polymer stability plays an important role in the positional regulation of FtsZ. *J Bacteriol* **183:** 5449–5452.

Lindow, J.C., Kuwano, M., Moriya, S., and Grossman, A.D. (2002) Subcellular localization of the *Bacillus subtilis* structural maintenance of chromosomes (SMC) protein. *Mol Microbiol* **46:** 997–1009.

Low, H.H., Moncrieffe, M.C., and Lowe, J. (2004) The crystal structure of ZapA and its modulation of FtsZ polymerisation. *J Mol Biol* **341:** 839–852.

Lutkenhaus, J.F., and Donachie, W.D. (1979) Identification of the *ftsA* gene product. *J Bacteriol* **137:** 1088–1094.

Ma, X., and Margolin, W. (1999) Genetic and functional analyses of the conserved C-terminal core domain of *Escherichia coli* FtsZ. *J Bacteriol* **181:** 7531–7544.

Marston, A.L., Thomaides, H.B., Edwards, D.H., Sharpe, M.E., and Errington, J. (1998) Polar localization of the MinD protein of *Bacillus subtilis* and its role in selection of the mid-cell division site. *Genes Dev* **12:** 3419–3430.

Michie, K.A., Monahan, L.G., Beech, P.L., and Harry, E.J. (2006) Trapping of a spiral-like intermediate of the bacterial cytokinetic protein FtsZ. *J Bacteriol* **188:** 1680–1690.

Miyagishima, S.Y., Wolk, C.P., and Osteryoung, K.W. (2005) Identification of cyanobacterial cell division genes by comparative and mutational analyses. *Mol Microbiol* **56:** 126–143.

Morimoto, T., Loh, P.C., Hirai, T., Asai, K., Kobayashi, K., Moriya, S., and Ogasawara, N. (2002) Six GTP-binding proteins of the Era/Obg family are essential for cell growth in *Bacillus subtilis*. *Microbiology* **148:** 3539–3552.

Moriya, S., Kato, K., Yoshikawa, H., and Ogasawara, N. (1990) Isolation of a *dnaA* mutant of *Bacillus subtilis* defective in initiation of replication: amount of DnaA protein determines cells' initiation potential. *EMBO J* **9:** 2905–2910.

Mosyak, L., Zhang, Y., Glasfeld, E., Haney, S., Stahl, M., Seehra, J., and Somers, W.S. (2000) The bacterial cell-division protein ZipA and its interaction with an FtsZ fragment revealed by X-ray crystallography. *EMBO J* **19:** 3179–3191.

Pichoff, S., and Lutkenhaus, J. (2002) Unique and overlapping roles for ZipA and FtsA in septal ring assembly in *Escherichia coli*. *EMBO J* **21:** 685–693.

Price, K.D., and Losick, R. (1999) A four-dimensional view of assembly of a morphogenetic protein during sporulation in *Bacillus subtilis*. *J Bacteriol* **181:** 781–790.

Rico, A.I., Garcia-Ovalle, M., Mingorance, J., and Vicente, M. (2004) Role of two essential domains of *Escherichia coli* FtsA in localization and progression of the division ring. *Mol Microbiol* **53:** 1359–1371.

Romberg, L., and Levin, P.A. (2003) Assembly dynamics of the bacterial cell division protein FTSZ: poised at the edge of stability. *Annu Rev Microbiol* **57:** 125–154.

Rozen, S., and Skaletsky, H. (2000) Primer3 on the WWW for general users and for biologist programmers. *Methods Mol Biol* **132:** 365–386.

Sackett, M.J., Kelly, A.J., and Brun, Y.V. (1998) Ordered expression of *ftsQA* and *ftsZ* during the *Caulobacter crescentus* cell cycle. *Mol Microbiol* **28:** 421–434.

Uchiyama, I. (2003) MBGD: microbial genome database for comparative analysis. *Nucleic Acids Res* **31:** 58–62.

Vagner, V., Dervyn, E., and Ehrlich, S.D. (1998) A vector for systematic gene inactivation in *Bacillus subtilis*. *Microbiology* **144:** 3097–3104.

Vasilescu, J., Guo, X., and Kast, J. (2004) Identification of protein–protein interactions using *in vivo* cross-linking and mass spectrometry. *Proteomics* **4:** 3845–3854.

Wang, X., Huang, J., Mukherjee, A., Cao, C., and Lutkenhaus, J. (1997) Analysis of the interaction of FtsZ with itself, GTP, and FtsA. *J Bacteriol* **179:** 5551–5559.

Yim, L., Vandenbussche, G., Mingorance, J., Rueda, S., Casanova, M., Ruysschaert, J.M., and Vicente, M. (2000) Role of the carboxy terminus of *Escherichia coli* FtsA in

self interaction and cell division. *J Bacteriol* **182:** 6366–6373.

Supplementary material

The following supplementary material is available for this article online:

Fig. S1. Amount of EzrA-, FtsA-, FtsZ-, YlmF- and ZapA-His proteins in the *B. subtilis* mutants.
Table S1. Primers used in this study.

This material is available as part of the online article from http://www.blackwell-synergy.com